JOURNAL OF MECHANICS OF CONTINUA AND MATHEMATICAL SCIENCES
www.journalimcms.org

ISSN (Online) : 2454 -7190 Vol.-21, No.-06, June (2026) pp 22-33 ISSN (Print) 0973-8975

EIGHT NODED FINITE ELEMENT APPROACH FOR ACOUSTIC EIGEN MODES OF MULTI CONNECTED REGIONS

K. Lekhana[1], K. T. Shivaram[2]

[1,2] Department of Mathematics, Dayananda Sagar College of Engineering, Visvesvaraya Technological University, Bangalore, India.

Email: [1]lekhanakailas26@gmail.com, [2]shivaramktshiv@gmail.com

Corresponding Author: **K. T. Shivaram**

https://doi.org/10.26782/jmcms.2026.06.00002

(Received: March 13, 2026; Revised: June 04, 2026; Accepted: June 14, 2026)

Abstract

This work uses the eight-noded quadrilateral finite element method to study the eigen analysis for several energy issues in the multiply-connected domain. The computing of eigenvalues across circular and multiply-connected curved domains is one of its applications, this method makes advantage of an excellent, eight-noded, quadrilateral automatic mesh generator created with MAPLE-18 software, this method makes use of a superb FEM process as seen by the examples provided, the proposed technique provides efficient numerical solutions for a range of problems and increases the accuracy of the numerical solution of eigenvalues that occur in a number of electromagnetic applications due to the reduced curvature loss, the validity of the current concept is demonstrated by these issues, the numerical results for the example situations using the suggested approach are quite similar to the best-published results.

Keywords: Eight-node, Mesh, Multi-connected regions, FEM, Helmoltz equation.

I. Introduction

The computer treatment of waveguides with arbitrary cross sections is a difficult problem, although there are many other methods for resolving this issue in the literature. Two things that they could lack are simplicity and quickness in order to simulate waveguides with any cross-section. For instance, handling waveguides with nonrectangular cross sections using the finite difference approach might be quite challenging. Here, the relevance of the problem's generality in explaining the usage of the eight noded quadrilateral finite element approach to solve for the waveguide cutoff wavenumbers, waveguides are employed anywhere high-frequency electromagnetic wave propagation is occurring in circular waveguides are defined as waveguides having a circular cross-section, waveguides are helpful for guiding and moving electromagnetic waves from one location to another, including microwaves, infrared waves, and radiofrequency waves, electromagnetic waves propagate through a variety of waveguide types, and the waveguide material, cut-off frequency, mode of

propagation and cross-section are some of the factors that go into choosing one, Typically, circular waveguide modes are variations of the transverse magnetic (TM) and transverse electric (TE) modes, each mode's field distribution changes in response to the circular waveguide's radial and circumferential fluctuations in TE and TM modes are supported by circular waveguides, which have a circular cross-section and circular waveguides are simpler to build than rectangular waveguides. However, for the reasons listed below, circular waveguides are less preferred than rectangular waveguides in frequency difference between the next mode and the lowest frequency of the dominant mode is less in a circular waveguide than in a rectangular one, For the specified operating frequency the circular waveguide's dimension is greater than the rectangular one, different circular waveguide modes and cut-off frequencies are needed for each application, circular waveguides are used in phase-shifters, radar systems, attenuators, antennas, and more, the application specifications are used to design the circular waveguide radius in addition to circular waveguides and design of waveguides of any cross-section, Higher order FEM's significance and application in computational electromagnetics are discussed in [XIV], In order to determine the eigenvalues and eigenmodes of the Helmholtz equation for 2-D and 3-D domains of any shape used byTai and Shaw [XV], this approach was also used to rectangular and circular geometries by De Mey [IV], Adeyeye et al. [I] computed the initial eigenvalue for a few circular, square and elliptic domains using three numerical techniques for the BEA of the Helmholtz equation under Dirichlet BC's., to get the Helmholtz eigenvalues in 2D and 3D using BEM and LU-decomposition by Kamiya et al. [VI–VIII], Lin [XII] used the cylindrical wave function transformation technique to satisfying the BC's for determining the eigenvalues of a circular domain with seven equal holes and an eccentric annular domain, The point-matching method was employed by Nagaya and Poltorak [XIII] to determine the eigenvalues of a circular domain with circular eccentric inner boundries, Both the FECM and point-matching methodology were employed by Nagaya and Yamaguchi [V] to determine the eigenvalues of the polygonal and elliptical outer boundary with circular eccentric inner boundaries, Chen [V] determined the eigenvalue and eigenmode for the multiply-connected wave guiding area using the BEM, Shivaram [II-III,IX-XI] recently used FEM to get the eigenvalue for the arbitrary polygonal and circular domain with four nodes and eight noded quadrilateral mesh.

FEM for waveguides has the following benefits:

- FEM can identify solutions for waveguides of any shape, unlike analytical approaches that are restricted to basic geometries like circular regions.
- By simply allocating distinct material characteristics to various mesh components, FEM can effortlessly manage waveguides with an uneven or composite material filling.
- The FEM solution may be brought arbitrarily near to the precise analytical solution by employing higher-order shape functions or a finer mesh.

A waveguide's eigenfrequencies have a major impact on how well electromagnetic waves propagate through it, according to studies. It is crucial to ascertain the waveguide's eigenfrequencies when electromagnetic waves with particular frequencies need to travel in a predetermined path. Our research aimed to examine the distinctive

frequencies that determine the precise wavelength at which various waveguides resonate by comparing waveguides of various forms. The eigenfrequencies of waveguides have been the subject of much investigation in the past by several scholars. Numerous numerical techniques have been presented to solve eigenproblems; they may be broadly categorized as mesh generation methods and meshfree approaches. A growing percentage of researchers favor analytical and numerical approaches. As computer technology has advanced, several numerical techniques have been created to address challenging engineering science issues. The eigen frequency problems of electromagnetic waves governed by two-dimensional Helmholtz equations with computational domains were solved in this study using the eight-noded quadrilateral finite element method, which was based on our knowledge of prior research on the eigen frequencies of waveguides and numerous numerical techniques. Furthermore, problems with complex domains, including multi-connected domains, might be correctly and rapidly analyzed using the suggested technique. Compare the outcomes with Chen [V] while utilizing the current method with an eight-noded FEM to determine the eigenvalue in multiconnected regions. This study presents an effective and straightforward method for dealing with challenges. Additionally, it offers the most accurate answers to some energy-related issues over 2D curved domains. This method can be used to address many more electromagnetic problems, and there are no analytical solutions for these types of circular domains. The potential results of the current approach can be compared to research papers, Chen [V].

II. Multi-connected circular waveguides

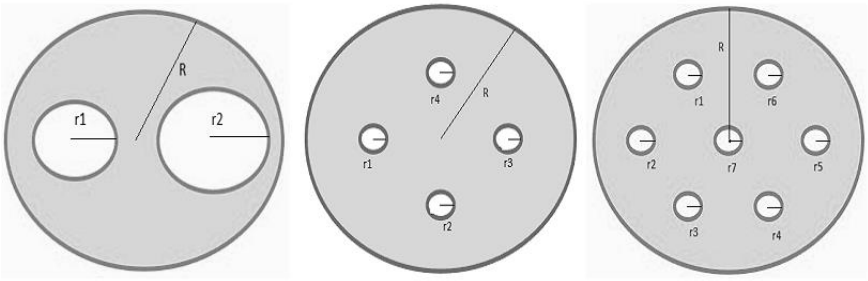

(a) (b) (c)

Fig. 1. a) Two uneven holes, b) Four equal holes, c) Seven equal holes in a circular wave guide

Figure 1 shows three different types of waveguides in a circular domain with an outer boundary radius of R = 1. Two circular inner boundaries with eccentricity of 0.5 are depicted in Figure 1a, with radii of r1 = 0.3 and r2 = 0.4, respectively. Four equal circular inner boundaries are shown in Figure 1b, with radii of 0.1, and four centers of the circular inner boundary are located at (0.5, 0), (-0.5, 0), (0, 0.5), (0, -0.5) respectively, Figure 1c. seven equal circular inner boundaries with radii of 0.1, the seven centers of the circular inner boundary are located at center (0, 0), (0.65, 0), (-0.65, 0), (0.3, 0.5), (0.3,0.5), (-0.3, -0.5), (0.3, -0.5) respectively, all three types of waveguides have Dirichlet-type boundary conditions (u = 0), to determine the eigenvalues for the multiply-connected issue, numerical experiments were carried out

for three scenarios. In the literature, multiply-connected domains' inner limits were constructed using the same geometry. To understand how inner boundary geometry impacts the eigenvalue, we constructed an example of a circular domain with two unequal inner holes. In order to compare them with alternative methods, the scenarios of a circular domain with four and seven equal holes were tested,

III. Eight-node Quadrilateral Elements

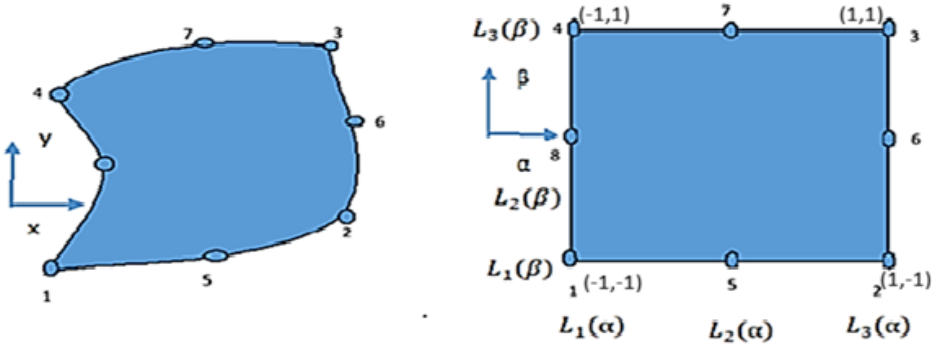

Fig. 2. Transformation of the xy- plane to the square αβ- plane

The eight-noded quadrilaterals have been proven to be quite effective in finite element analysis. It is possible to determine the shape function of an eight-node rectangular element like that of a four-node element. Since this element is quadratic in nature, the only change will be in the polynomial that is chosen. If the Cartesian coordinate system is used, the derivation will be algebraically complicated. However, because the element's natural coordinates range from -1 to +1,

The following polynomial can be used to express the variation of the field variable ϕ in the natural coordinate system.

The shape functions of the Q8 element cover a greater area of the Pascal triangle than those of Q4, Q4 covers the bilinear space V = span{1, α, β, αβ } of degree 1, while Q8 covers the serendipity space V = span{1, α, β, α^2, αβ, β^2, $\alpha^2\beta$, $\alpha\beta^2$ } of degree 2, then

$$\Phi(\alpha,\beta) = a_0 + a_1\alpha + a_2\beta + a_3\alpha^2 + a_4\alpha\beta + a_5\beta^2 + +a_6\alpha^2\beta + a_7\alpha\beta^2 \qquad (1)$$

The coordinates at nodes are entered into the above expression, and the nodal field variables can be derived by using the natural coordinate system, which will simplify the procedure. The local node counts for these elements are presented in Figure 2b. In terms of the natural coordinates α and β, the Lagrange interpolation functions for the eight-node rectangular element are provided by Sabine [XIV]

$$N_i = \frac{1}{4}\begin{bmatrix} (1-\alpha)(1-\beta)(-\alpha-\beta-1) \\ (1+\alpha)(1-\beta)(\alpha-\beta-1) \\ (1+\alpha)(1+\beta)(\alpha+\beta-1) \\ (1-\alpha)(1+\beta)(-\alpha+\beta-1) \\ 2(1-\alpha^2)(1-\beta) \\ 2(1+\alpha)(1-\beta^2) \\ 2(1-\alpha^2)(1+\beta) \\ 2(1-\alpha)(1-\beta^2) \end{bmatrix} \qquad (2)$$

Where N_i is the Lagrange interpolation function at node $i = 1\ to\ 8$
The interpolation functions can be used to express an element's geometry as follows:

$$x = \sum_{i=1}^{8} x_i N_i(\alpha, \beta) \text{ and } y = \sum_{i=1}^{8} y_i N_i(\alpha, \beta) \tag{3}$$

$$\frac{\partial x}{\partial \alpha} = \sum_{i=1}^{8} \frac{\partial N_i}{\partial \alpha} x_i , \quad \frac{\partial x}{\partial \beta} = \sum_{i=1}^{8} \frac{\partial N_i}{\partial \beta} x_i$$

$$\text{and } \frac{\partial y}{\partial \alpha} = \sum_{i=1}^{8} \frac{\partial N_i}{\partial \alpha} y_i , \quad \frac{\partial y}{\partial \beta} = \sum_{i=1}^{8} \frac{\partial N_i}{\partial \beta} y_i$$

$$\begin{pmatrix} \frac{\partial N_i}{\partial \alpha} \\ \frac{\partial N_i}{\partial \beta} \end{pmatrix} = \begin{bmatrix} \frac{\partial x}{\partial \alpha} & \frac{\partial y}{\partial \alpha} \\ \frac{\partial x}{\partial \beta} & \frac{\partial y}{\partial \beta} \end{bmatrix} \begin{pmatrix} \frac{\partial N_i}{\partial x} \\ \frac{\partial N_i}{\partial y} \end{pmatrix} = J \begin{pmatrix} \frac{\partial N_i}{\partial x} \\ \frac{\partial N_i}{\partial y} \end{pmatrix}$$

$$\begin{pmatrix} \frac{\partial N_i}{\partial x} \\ \frac{\partial N_i}{\partial y} \end{pmatrix} = J^{-1} \begin{pmatrix} \frac{\partial N_i}{\partial \alpha} \\ \frac{\partial N_i}{\partial \beta} \end{pmatrix} \tag{4}$$

IV. Mesh creation in a multiconnected with circular region

To build a class of suitable triangular meshes in order to attain the optimal rate of convergence for the finite element solution when the corner singularity is present in the solution of equation (5). Starting with an initial triangulation of Δ, we divide each triangle into four triangles to produce such a sequence of triangulations, which is analogous to the conventional midpoint refinement. Every triangle is divided into three sub-eight-noded quadrilaterals, and the Jacobian is unique for these three eight-noded quadrilaterals. The difference is that, as we refine, we move the middle points of edges in the direction of the unique vertex of Δ in order to target the corner singularity in a single vertex V_i, the quadratic approximation is made possible by the point distribution within each of the collection of triangular subregions that make up the circular multiconnected guiding cross-section. This is really beneficial since, in contrast to linear approximation, we can represent the boundary shape with a small number of triangles, which will lead to accuracy. Each triangle is further divided into eight-noded three-quadrilateral parts. An autonomous eight-noded mesh generator was used to mesh the waveguide cross-section, as shown in Figure 3. The large, dense mesh needed for the 4-node model actually takes longer for a computer to solve than the clever, effective 8-node mesh.

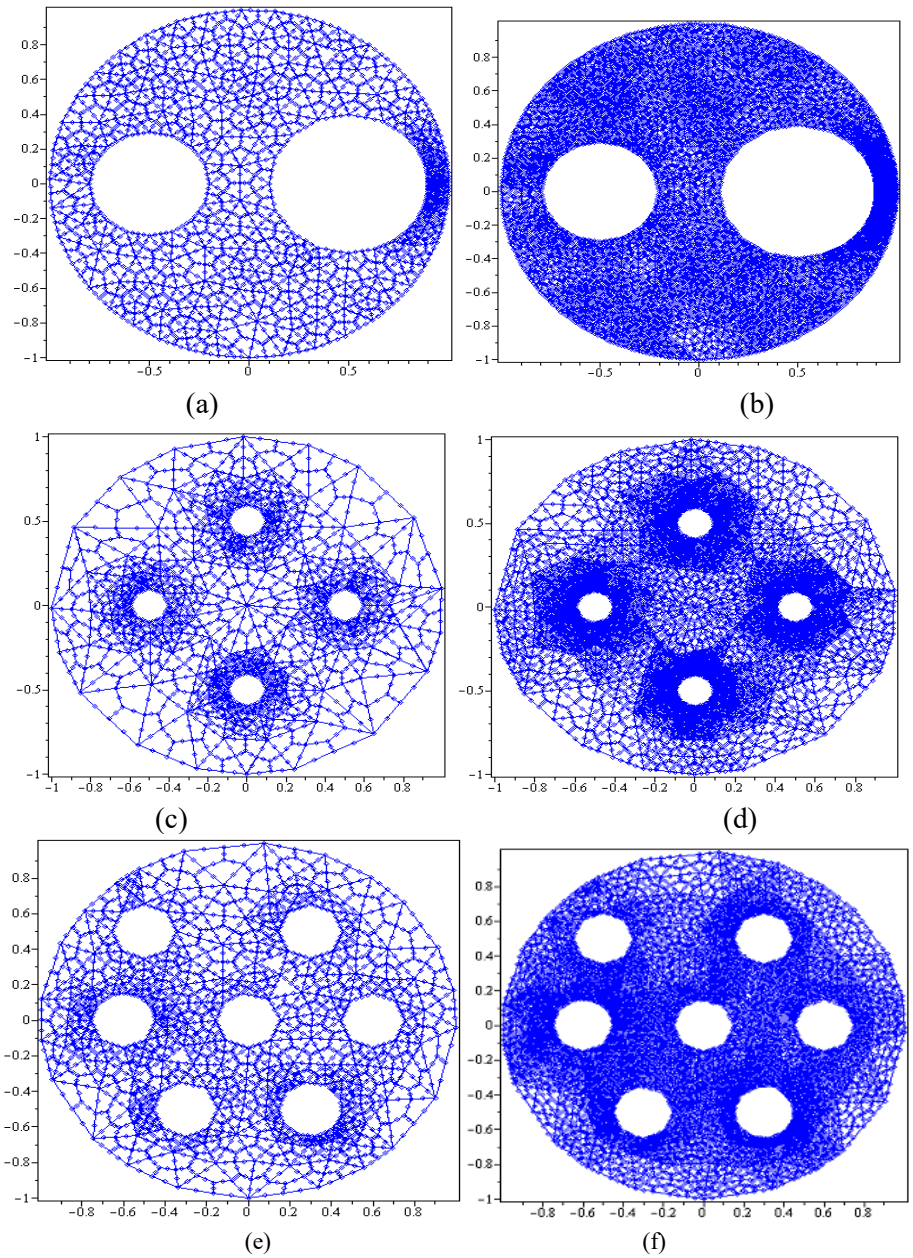

Fig. 3. Auto mesh generation over equal and unequal holes in a circular region

The distance between the inner and outer limits narrows on one side when an inner circular boundary is pushed eccentrically. In doing so, the curved eight-node elements are stretched and compressed. For the worst-case components, we compute a common measure known as the Jacobian Ratio to assess this distortion.

$$Jacobian\ ratio = \frac{Min \det(J)}{Max \det(J)}$$

If this ratio remains at zero, it indicates that the elements are not overly distorted to produce correct results and that the mapping quality is excellent.
For a geometric transformation to be deemed non-singular, it must never invert, fold over itself, or collapse into a zero-area shape. The results show that the computed eigenvalues softly converge to the correct, stable number, even when the mesh becomes considerably distorted, by looking at the determinant of the Jacobian matrix det(J) at each integration point across all curved elements. Because the results don't fluctuate significantly, we can confidently state that our strategy is stable.

V. Scalar formulation for homogeneous waveguides using an eight-node finite element technique

This section presents the Helmholtz equation mathematically using the mesh generators from section (4) and the suggested eight-noded quadrilateral FEM technique. The 2D Helmholtz equation is provided by:

$$\nabla^2\omega + A_c^2\omega = 0 \tag{5}$$

each waveguide's wavenumbers A_c are determined by taking the square root of its eigenvalues, which are computed in the conventional matrix form. Similarly, the cutoff wave number is the lowest wavenumber. The following list of various unknowns derived from the matrix form is available in Adeyeye [I]. The Helmholtz equation is transformed into matrix form upon application of the Galerkin finite element formulation; the specifics of this transformation are completed in our earlier work. Shivaram [X]

$$[C + D]_{KXK} * [\omega]_{KX1} = [0]_{KX1} \tag{6}$$

For convenience, the unknowns in the stiffness matrix are given below and are precisely specified in Yogitha [II].

$$C_{r_1,r_2} = C_{x_1,x_1}^{r_1,r_2} + C_{x_2,x_2}^{r_1,r_2} \tag{7}$$

$$C_{x_1,x_1}^{r_1,r_2} = \int_{-1}^{1}\int_{-1}^{1} \frac{1}{j} \begin{vmatrix} \frac{\partial N_{r_1}}{\partial \alpha} & \frac{\partial N_{r_1}}{\partial \beta} \\ \frac{\partial x_1}{\partial \alpha} & \frac{\partial x_1}{\partial \beta} \end{vmatrix} * \begin{vmatrix} \frac{\partial N_{r_2}}{\partial \alpha} & \frac{\partial N_{r_2}}{\partial \beta} \\ \frac{\partial x_1}{\partial \alpha} & \frac{\partial x_1}{\partial \beta} \end{vmatrix} d\alpha d\beta$$

$$C_{x_2,x_2}^{r_1,r_2} = \int_{-1}^{1}\int_{-1}^{1} \frac{1}{j} \begin{vmatrix} \frac{\partial N_{r_1}}{\partial \alpha} & \frac{\partial N_{r_1}}{\partial \beta} \\ \frac{\partial x_2}{\partial \alpha} & \frac{\partial x_2}{\partial \beta} \end{vmatrix} * \begin{vmatrix} \frac{\partial N_{r_2}}{\partial \alpha} & \frac{\partial N_{r_2}}{\partial \beta} \\ \frac{\partial x_2}{\partial \alpha} & \frac{\partial x_2}{\partial \beta} \end{vmatrix} d\alpha d\beta$$

$$D = \int_{\omega_e} A_c^2 N_{r_1} N_{r_2} dxdy$$

When waveguides have a regular geometry, the GLQ rule of order N=5 is used to do the aforementioned integration.

If h is the element size, the precision of a 4-Node element Q4 increases at a rate of $O(h^2)$ inaccuracy decreases to 1/4 if you cut the element size in half. For our 8-Node Element Q8, the accuracy increases at a rate of $O(h^2)$. Inaccuracy decreases to 1/16 if

you cut the element size in half. The condition number rises when the mesh is refined in several FEM techniques. $O(h^2)$, where h is the element size numerically, if the present method prevents the iteration count k from exploding by maintaining the condition number constant even while holes are introduced.

VI. Results and discussion

6.1 Two uneven holes in a circular wave guide

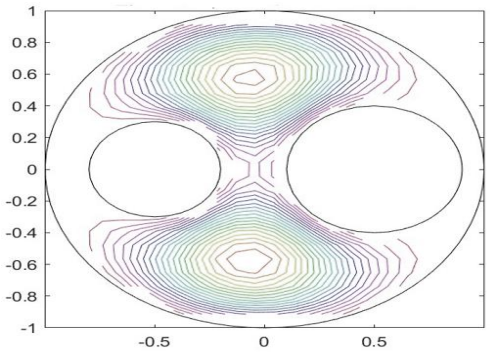

Fig. 4. First eigenvalue $A_1 = 4.82248$ of circular waveguide with two uneven holes (TM mode)

This domain is the same as that of Chen [V] for a circular waveguide with two unequal holes. Over the waveguide cross-section, the domain is separated into 414 and 1656 eight-noded quadrilateral elements for the two scenarios. The Dirichlet boundary condition is taken into consideration, as seen in Figures 3a and 3b. The top five eigenvalues produced using the current approach are displayed in Table 1. The size of the computational matrix for the 414 and 1656 eight-noded quadratic cases is 97x97 and 388x388. The difference between the cutoff wavenumber obtained in the present case and Chen [V] is 0.001%. Using the boundary element method to determine the eigenvalue, a numerical result is observed with convergence in Chen [V]. This is reported in Table 1. The eight-noded quadratic elements 414 and 1656 have cutoff wavenumbers of 4.82034 and 4.82248, respectively, and are shown in Figure 4. When the order of discretization from 414 to 1656 eight-node quadrilateral elements is examined, a good convergence is shown

Table 1: Cutoff wave number of a two uneven holes in a circular wave guide

Eigenvalue in TM mode A_C	BEM [10]	FEM [10]	Present method For mesh 1a Elements=414	Present method For mesh 1b Elements=1656
A_1	4.82	4.790	4.82034	4.82248
A_2	4.82	4.801	4.81446	4.82064
A_3	6.72	6.619	6.71518	6.72144
A_4	6.72	6.634	6.69330	6.72410
A_5	7.82	7.792	7.79732	7.80327

6.2 Four identical holes in a circular wave guide

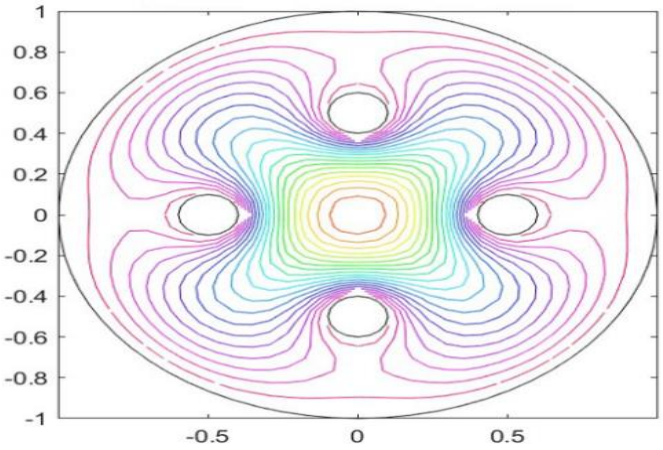

Fig.5. First eigenvalue $A_1 = 4.46180$ of circular waveguide with four even holes (TM mode)

The circular waveguide in Chen [V] has four equal holes. The domain in this instance is separated into an eight-noded quadratic. Table 2 shows the eigenvalues for the first five that were determined using the current method. In this instance, it is evident that a decent convergence is achieved with 617 and 1144 eight-noded quadrilateral elements; the precision is achieved using BEM in Chen [V] in a manner comparable to the current approach. The cutoff wavenumber derived with 617 and 1144 items has a difference (%) of 0.03% with Chen [V], the meshes utilized in this instance, and compared with the first eigenvalue $A_1 = 4.46180$ and plotted in Figure 5. Since a tiny eight-noded quadratic mesh is employed in this instance, processing time and effort will be comparatively minimal.

Table 2: Cutoff wave number of a four even holes in a circular wave guide

Eigenvalue in TM mode A_C	BEM Chen [V]	FEM Chen [V]	Present method for mesh 1a Elements =617	Present method for mesh 1b Elements =1144
A_1	4.47	4.443	4.43178	4.46180
A_2	5.37	5.316	5.34409	5.37659
A_3	5.37	5.320	5.33381	5.33381
A_4	5.54	5.486	5.53283	5.54465
A_5	5.95	5.884	5.91350	5.93613

6.3 Seven identical holes in a circular wave guide

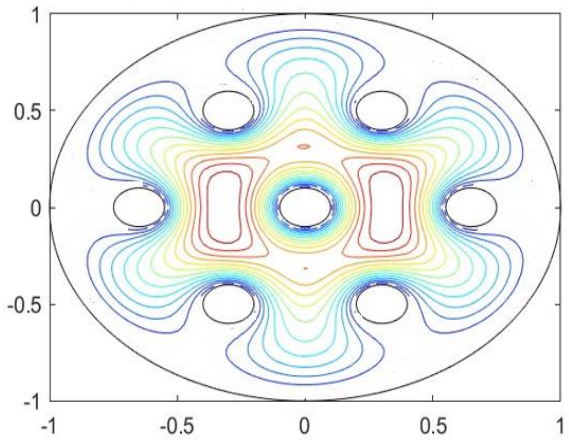

Fig. 6. First eigenvalue $A_1 = 4.46180$ of circular waveguide with seven even holes (TM mode)

Two kinds of discretization are used to compare the rate of cutoff wavenumbers. It should be mentioned that because the solution does not converge well at lower orders, higher-order discretization is necessary for circular geometries. Figure 6 depicts the waveguide's domain under consideration. There are seven equal holes in the circular waveguide in Chen [V]. In this case, the domain is divided into eight-noded quadratic elements. The results are shown in Table 3. It is clear that a respectable convergence is attained in this case; the precision is attained using BEM in a way similar to the current method, with 1370 and 2568 eight-noded elements. The cutoff wavenumber calculated with 1370 and 2568 elements has a difference (%) of 0.04% with Chen [V] in the current technique.

Table 3: Cutoff wave number of a seven even holes in a circular wave guide

Eigenvalue in TM mode A_C	BEM Chen [V]	FEM Chen [V]	Present method For mesh 3e Elements=1370	Present method For mesh 3f Elements=2568
A_1	7.68	7.533	7.6277	7.6433
A_2	8.01	7.821	7.9851	7.9983
A_3	8.01	7.828	7.9849	7.9995
A_4	8.34	8.100	8.2503	8.3154
A_5	8.34	8.106	8.2591	8.3198

VII. Conclusions

In order to effectively and precisely study the eigenfrequency problems, which were controlled by the two-dimensional Helmholtz equation, this paper developed an eight-noded quadrilateral FE mesh generating method. The application and effectiveness of the eight-noded Galerkin finite element numerical method were confirmed in our study by examining two, four, and seven equal and unequal inner radii

in a multi-connected domain waveguide. The external source's position was not fixed as long as it was outside the computational domain. This current numerical method can be used to determine a waveguide's characteristic wavelength, and its accuracy can be confirmed by testing various scenarios. The suggested eight-noded quadrilateral FE mesh generation technique was demonstrated to be able to handle a complex computational domain in practical engineering applications. Additionally, the accuracy and computing efficiency were demonstrated.

Conflict of Interest:

There was no relevant conflict of interest regarding this paper.

References

I. Adeyeye, J. O., Bernal, M.J.M., & Pitman, K. E. (1985). An improved boundary integral equation method for Helmholtz problems. Internatinal Journal for Numerical Methods in Engineering, 21(1), 779–787. 10.1002/nme.1620210502

II. Yogitha, A. M., Shivaram, K. T., Rajesh, S. M., & Mahesh Kumar, N. (2024). Numerical computation of cut off wave number in polygonal wave guide by eight node finite element mesh generation approach, Journal of the Nigerian Society of Physical Sciences, 6(4), 1-6. 10.46481/jnsps.2024.2149

III. Yogitha, A. M., & Shivaram, K. T. (2025). A twelve noded finite element approximation to 2d- poisson equations with a dirac line source, Journal of Mechanics of Continua and Mathematical Sciences, 20(5), 26-37. 10.26782/jmcms.2025.05.00003

IV. De mey, G. A. (1977). Calculation of eigenvalues of the Helmholtz equation by an integral equation, International Journal for Numerical Methods in Engineering, 10(1), 59-66. 10.1002/nme.1620100105

V. Chen, J. T., Liu1, L. W., & Chyuan, S. W. (2004). Acoustic eigenanalysis for multiply-connected problems using dual BEM, Communications in numerical methods in engineering, 20(1), 419–440. 10.1002/cnm.679

VI. Kamiya, N., Andoh, E., & Nogae, K. (1993). Three-dimensional eigenvalue analysis of the Helmholtz equation by multiple reciprocity boundary element method, Advances in Engineering Software, 16(3), 203–207. https://www.sciencedirect.com/science/article/abs/pii/096599789390018O

VII. Kamiya, N., & Andoh, E. (1993). Helmholtz eigenvalue analysis by boundary-element method, Journal of Sound and Vibration, 160(2), 279–287. 10.1006/jsvi.1993.1023

VIII. Kamiya, N., & Andoh, E. (1993). Eigenvalue analysis by the boundary element method: new developments, 12(3), 151-162. 10.1016/0955-7997(93)90011-9

IX. Lekhana, K., & Shivaram, K. T. (2025). A method for creating twelve-node finite element meshes to find the cutoff wave number for polygonal and circular waveguides, International Journal of Basic and Applied Sciences, 14(1), 59-64. 10.14419/y9648s16

X. Shivaram, K. T., & Jyothi, H. R.(2021). Finite element approach for numerical integration over family of eight node linear quadrilateral element for solving Laplace equation, Materials Today Proceedings, 46(9), 4336-4340. 10.1016/j.matpr.2021.03.437

XI. Shivaram, K. T., Harshitha,L. M. P., Chethana, H. P., & Nidhi, K. (2018). Finite element mesh generation technique for numerical computation of cutoff wave numbers in rectangular and L-shaped wave- guide, 3rd International Conference on Inventive Computation Technologies (ICICT), IEEE Xplore,704-706. 10.1109/ICICT43934.2018.9034432

XII. Lin, W. H. (1981). Guided waves in a circular duct containing an assembly of circular cylinders, Journal of Sound and Vibration, 79(4), 463–477. 10.1016/0022-460X(81)90460-0

XIII. Nagaya, K., & Poltorak, K. (1989). Method for solving eigenvalue problems of the Helmholtz equation with a circular outer and a number of eccentric circular inner boundaries, Journal of the Acoustical Society of America, 85(2), 576–581. 10.1121/1.397581

XIV. Sabine Zaglmayr, High order finite element methods for electronic field computation, Ph.D thesis. 2006. https://www.numerik.math.tugraz.at/~zaglmayr/pub/szthesis.pdf

XV. Tai, G. R. C., & Shaw, R. P. (1974). Helmholtz equation eigenvalues and eigenmodes for arbitrary domains, Journal of the Acoustical Society of America, 56(3), 796-804. 10.1121/1.1903328